

Technical Note

Behavior of rockfill materials in triaxial compression testing

A. Soroush^{1,*}, R. Jannatiaghdam²

Received: March 2010, Revised: February 2011, Accepted: October 2011

Abstract

This paper studies thoroughly and deeply the results of about one hundred triaxial compression tests on thirty types of rockfill materials. The materials are categorized in accordance with their particles shape (angular / rounded) and gradation characteristics. The main tool of the study is the Hyperbolic Model developed by Duncan and Chang. The focus of the study is on the variations of deformation modulus of the materials (E_i and E_v) with confining stress (σ_3). Features of the mechanical behavior of the rockfill materials, as compared with the general behavior of soils, are highlighted through the exponent parameter (n) of the Hyperbolic Model. It is shown that high confining stresses may have adverse effects on the deformation modulus of the rockfill materials and make them softer. The particle breakage phenomenon which happens during compression and shearing is found as the main factor responsible for the above effects and, in general, responsible for controlling the behavior of the materials. For the rockfill materials of this study, two correlations for estimating the initial elasticity modulus (E_i) and the internal friction angle (ϕ) in terms of particles shape, confining pressure (σ_3), and coefficient of uniformity (C_u) are suggested.

Keywords: Rockfill materials; Hyperbolic model; Triaxial test; Particle breakage; Deformation modulus; Internal friction angle.

1. Introduction

Rockfill materials are widely used in engineering structures, such as rockfill dams [1] and reclamation sites. Shear strength and deformation characteristics of rockfill materials depend on such parameters as their mineralogy, grain size distribution, size of particles and applied stress levels.

When thick layers of a rockfill material are subjected to high stresses (due to the weight of top layers), the material suffer particle breakage to some extents. This leads to changes in the material gradation, which results in changes in the mechanical behavior of the material.

The importance of particle breakage goes back to its capability of changing gradations of granular materials. All coarse materials which undergo stresses higher than normal ranges of geotechnical engineering, suffer particle breakage. Although breakage of particles of some special materials, such as carbonate sands [2, 3], can happen even due to low confining stresses, the stress level plays a major role in the

probability and amount of breakage. Stability and deformation behaviors of rockfill structures depend on the shear strength and deformation parameters of their materials. Marsal found that the shear strength of rockfill materials is directly related to their dry density, roughness, and breakage strength; also their strength is diversely related to sizes of particles and coefficient of uniformity (C_u) of the material [4].

Triaxial testing has been widely used to characterize the mechanical behavior of fine and coarse geomaterials under a variety of monotonic, cyclic, and post-cyclic loadings [2, 5, 6]. Medium and large scale triaxial apparatuses have been employed for rockfill materials.

This paper presents the results of a comprehensive study on the mechanical behavior of thirty rockfill materials under medium and large scale triaxial testing. Data about the materials and the tests are gathered from the literature. The Hyperbolic Model (HM) [7] is employed as an analytical and behavioral framework for this study. The important parameters of the HM for the rockfill materials are determined and compared with similar parameters for typical loose and dense sands. For each of the materials, variations of the deformation and strength parameters (E_i and ϕ) with confining stresses (σ_3) are studied. On the basis of this study, two relationships for estimating E_i and ϕ of the rockfill materials from triaxial compression testing results are proposed.

* Corresponding Author: Soroush @aut.ac.ir
1 Associate Professor, Department of Civil and Environmental Engineering, Amirkabir University of Technology, Tehran, Iran
2 M.Sc. Student, Department of Civil and Environmental Engineering, Amirkabir University of Technology, Tehran, Iran

2. Properties of the rockfill materials

Thirty types of rockfill materials, on which conventional triaxial compression tests had been carried out, are used in this study. The pre-test gradations of the materials are presented in Figures 1 and 2. The materials' characteristics, including mineralogy, uniformity coefficient, shape of particles and etc. are summarized in Table 1. This table is the main source of data employed in this research. The last column of the table introduces the references of the materials and tests data. The symbols used in Table 1 are all introduced at the end of the paper. A key symbol (B_g), however, is described here, as follows.

The value of B_g for a specimen subjected to a specific test is usually calculated by sieving the specimen materials using a set of sieves (50 to 0.075 mm) before and after the test. The

percentage of particles retained in each sieve is determined at both stages. After the test due to breakage of the particles, the percentage of the particles retained in large size sieves will decrease and the percentage of particles retained in small size sieves will increase. The sum of the decreases will be equal to the sum of the increases in the percentage retained. The decrease (or increase) is the value of the Breakage Index, B_g [4].

3. Hyperbolic Model and its Application

3.1. Theory of the Model

The Hyperbolic Model (Duncan & Chang [7]) considers the behavior of a soil specimen under compressive triaxial testing as a hyperbola. According to the model, the gradient of the

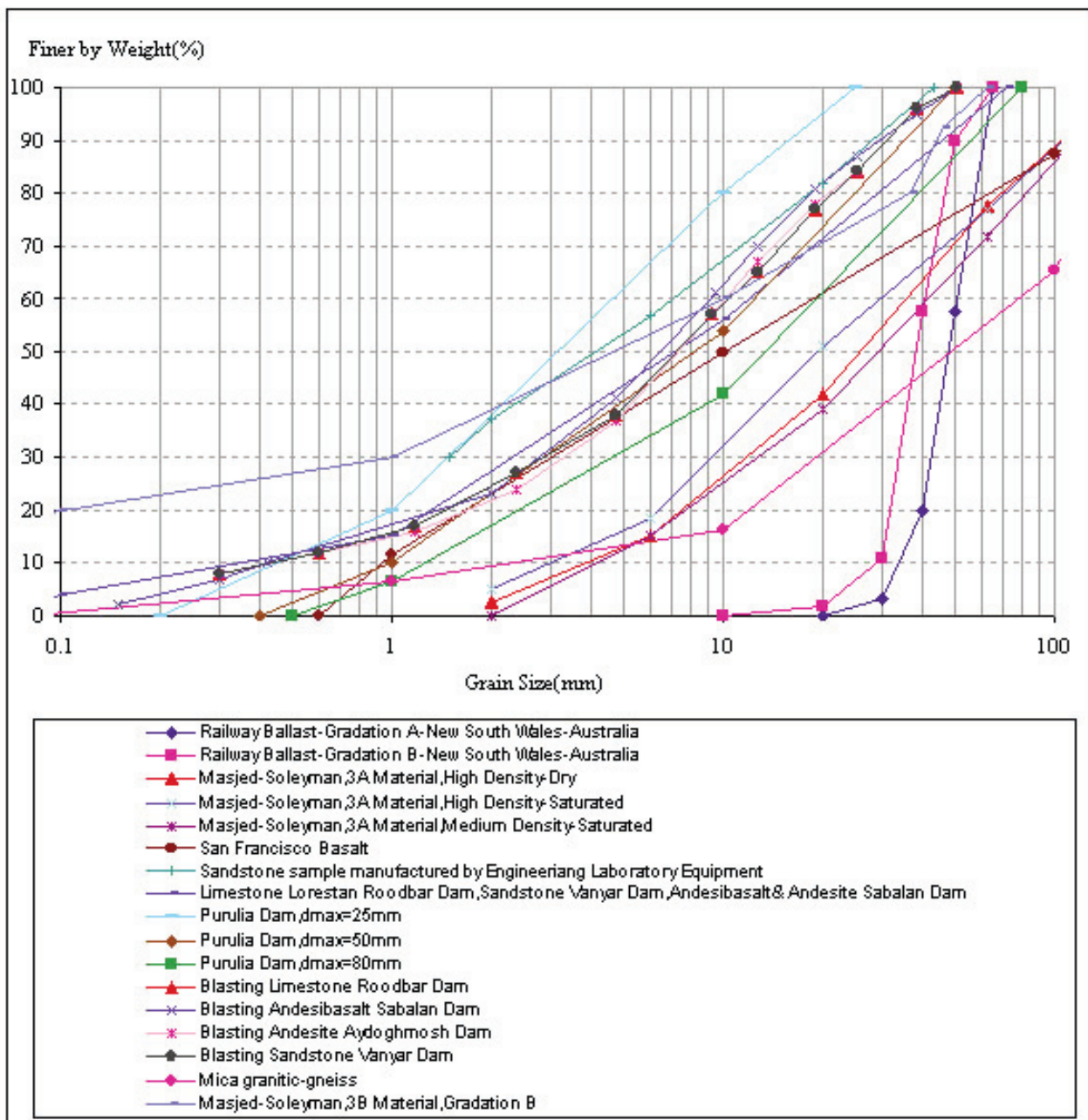


Fig. 1. Gradations of relatively angular materials

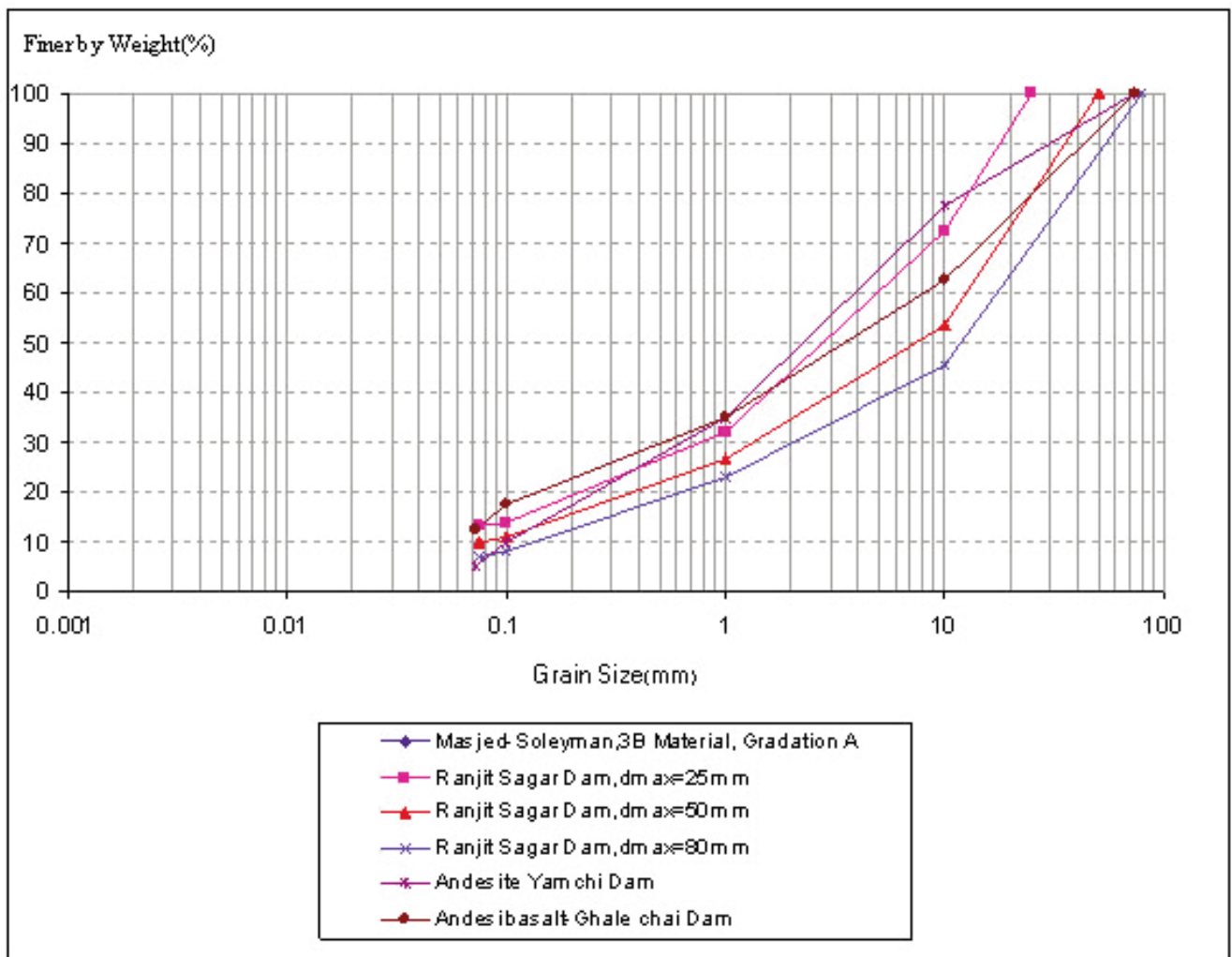


Fig. 2. Gradations of relatively rounded materials

tangent to the stress-strain relationship ($q:\epsilon_a$), namely the tangential deformation modulus (E_t), is defined as follows:

$$E_t = \left\{ 1 - \frac{R_f (1 - \sin\phi)(\sigma_1 - \sigma_3)}{2c \cos\phi + 2\sigma_3 \sin\phi} \right\}^2 E_i \quad (1)$$

Where,

ϕ : internal friction angle

c : cohesion

R_f : failure ratio, and

E_i : Initial elastic modulus, defined as [2].

$$E_i = KP_a \left(\frac{\sigma_3}{P_a} \right)^n \quad (2)$$

In which,

K : modulus number

n : exponent number, and

P_a : atmospheric pressure

The above parameters for a given soil can be obtained by carrying out, usually, three triaxial tests on the material's specimens.

3. 2. Application of the Hyperbolic Model

In this section, the mechanical parameters of the rockfill materials, introduced in Table 1, are investigated analytically in the framework of the Hyperbolic Model. Values of parameters n and K for every two consecutive triaxial tests, and furthermore, for three triaxial tests, conducted on each of the materials, are extracted and presented in Table 2. In other words, three values of n are calculated for each of the materials; one from the first and second triaxial tests results; one from the second and third triaxial tests results; and one from the first, second and third triaxial tests. We intentionally calculated the first two values of n in order to highlight the effect of particle breakage on E_i (through n) during every increase of σ_3 . This is different from the similar procedure of determining n for soils, where usually a unique n value is extracted from results of triaxial tests with three consecutive confining stresses (σ_3) on a given material. The procedure of determining n and K from the triaxial tests results are given in Duncan and Chang [7].

According to Table 2, the values of n vary between -7.45 and +2.70 for the studied rockfill materials. It can be realized that unlike for soils, n can have a negative value, which may not be

Table 1. Mechanical properties of the rockfill materials

Rockfill type	Mineralogy	d_{min} (mm)	d_{max} (mm)	C_u	σ_3 (kPa)	* ϕ°	** B_g (%)	Shape	Reference
Railway Ballast-Gradation A-New South Wales-Australia CD test	Latite basalt	20	65	1.5	90	54.6	10	Highly Angular	[14]
					120	52			
					240	45.8			
Railway Ballast-Gradation B-New South Wales-Australia CD test	Latite basalt	10	65	1.6	90	56.7	8.66	Highly Angular	[14]
					120	52.5			
					240	45.8			
Masjed-Soleyman,3A Material High Density-Dry CD test	Calcareous conglomerate	2	160	7.2	600	47	54.5	Angular	[11]
					1200	44	56		
					1800	42	65		
Masjed Soleyman,3A Material High Density-Saturated-CD test	Calcareous conglomerate	2	160	7.5	300	51	32	Angular	[11]
					600	47	49.5		
					1200	43	55.5		
Masjed Soleyman,3A Material Medium Density-Saturated-CD test	Calcareous conglomerate	2	150	8.95	300	45	23	Angular	[11]
					600	42	25		
					1200	41	29		
San Francisco Basalt Dry-CD test	Basalt	0.6	200	22.46	500	46.2	13.6	Angular	[4]
					1000	42.1	11.4		
					2500	38.3	12.6		
Sandstone sample manufactured by Engineering Laboratory Equipment Ltd. CD test	Sand stone	1.5	43.5	5.65	90	50	+NIA	Angular	[12]
					282	42			
					695	38.7			
Motorway Embankment Gneiss,Italy Dry-CD test	Gneiss	NIA	NIA	NIA	300	42	NIA	Angular	[13]
					500				
					1000				
Limestone Lorestan Roodbar Dam-CD test	Limestone	0.088	71.4	19.74	300	39	NIA	Angular	[17]
					500				
					700				
Sandstone Vanyar Dam-CD test	Sandstone	0.088	71.4	19.74	300	36	NIA	Angular	[17]
					500				
					700				
Andesibasalt& Andesite Sabalan Dam-CD Test	Andesi basalt &Andesite	4.667	71.4	19.74	300	41	NIA	Angular	[17]
					600				
					900				
Dolomite RailRoad Ballast,Coteau,Quebec, Canada- CD test	Dolomite	0.2	38.57	2.85	34.4	40	NIA	Angular	[15]
					51.7				
					310				
Purulia Dam Dry-CD test	Quartz,biotite, feldespar	0.4	25	16.37	300	32.5	1.4	Angular/sub Angular	[10]
					900		6		
					1200		8.0		
Purulia Dam Dry-CD test	Quartz,biotite, feldespar	0.5	50	16.66	300	31.4	2.2	Angular/sub Angular	[10]
					900		9.2		
					1200		12.6		
Purulia Dam Dry-CD test	Quartz,biotite, feldespar	0.15	80	17.14	300	30.6	3	Angular/sub Angular	[10]
					900		11		
					1200		15		
Blasting Lime stone Roodbar Dam CD test	Lime stone	0.15	50.8	23	500	30.6	11	Angular/sub Angular	[18]
					700		12		
					900		13.5		
Blasting Andesibasalt Sabalan Dam CD test	Andesibalast	0.15	50.8	22.1	300	42	5.5	Angular/Sub Angular	[18]
					600	40	10		
					900	40	14		
Blasting Andesite Aydoghmosh Dam CD test	Andesite	0.3	50.8	22.9	300	38	4	Angular/Sub Angular	[18]
					500	38	5		
					700	38	5		

Table 1. Mechanical properties of the rockfill materials (cont.)

Rockfill type	Mineralogy	d_{\min} (mm)	d_{\max} (mm)	C_u	σ_3 (kPa)	* φ°	** B_g (%)	Shape	Reference
Blasting Sandstone Vanyar Dam CD test	Sandstone	0.3	50.8	22.9	500 700	38 38	11 12	Angular/Sub Angular	[18]
Mica granitic- gneiss Dry-CD test	Granitic-gneiss	0.03	200	20.67	500 1000 2500	44.5 44 43	10.5 16.8 23.9	Sub Angular	[4]
Masjed -soleyman,3B Material CU Test, W_{opt} , Gradation B	Conglomerate and Sandstone	0.00175	62.5	1242	150 300 600	37.2 34 32.3	NIA	Sub Angular	[16]
Masjed- soleyman,3B Material CU Test, W_{opt} -2%, Gradation B	Conglomerate and Sandstone	0.00175	62.5	1242	150 300 600	49.8 44.7 42.0	NIA	Sub Angular	[16]
Masjed -soleyman,3B Material CD Test, Gradation A	Conglomerate and Sandstone	0.00175	62.5	1242	150 300 600	46.3 44.3 43.0	NIA	Sub Rounded	[16]
Masjed- soleyman,3B Material CU Test, W_{opt} , Gradation A	Conglomerate and Sandstone	0.00175	62.5	1242	150 300 600	46.2 45 42.7	NIA	Sub Rounded	[16]
Masjed- soleyman,3B Material CU Test, W_{opt} -2%, Gradation A	Conglomerate and Sandstone	0.00175	62.5	1242	150 300 600	50.0 43.7 43.1	NIA	Sub Rounded	[16]
Ranjit Sagar Dam Dry-CD test	Conglomerate, Sandstone	0.075	25	93.33	350 1100 1400	31.5	4 7 9	Rounded/Sub Rounded	[10]
Ranjit Sagar Dam Dry-CD test	Conglomerate, Sandstone	0.075	50	173.5	350 1100 1400	33.2	5 8.5 10	Rounded/Sub Rounded	[10]
Ranjit Sagar Dam Dry-CD test	Conglomerate, Sandstone	0.075	80	145.3	350 1100 1400	35.4	6 9.6 12	Rounded/Sub Rounded	[10]
Andesite Yamchi Dam-CD test	Andesite	0.072	74.3	65.4	200 400 700	38.7	NIA	Rounded	[17]
Andesibasalt Ghale chai Dam CD test	Andesibasalt	0.072	74.3	138.9	400 700	36.5	NIA	Rounded	[17]

* φ is calculated for each triaxial test, assuming $c=0$

** B_g : Marsal's breakage index

†NIA : No Information Available

unique for a specific rockfill material with a given relative density; in fact, n varies with confining pressure ranges. Interestingly, a considerable number of n values are negative, which implies the decrease of E_i with the increase of confining pressure (σ_3). The reason for this behavior is the occurrence of particle breakage, which changes the materials' gradations and influences their behavior.

Figure 3 shows the statistical variations of n for the studied rockfill specimens in (a) the first stage of confining pressure increasing (with a range of σ_3 between 34.4 kPa and 1200 kPa) and (b) the second stage of confining pressure increasing

(with a range of σ_3 between 51.7 kPa and 2500kPa). It is observed that n has taken a wide range of values. Of course, the value of n and its sign (+ve versus -ve) depends on several material and loading factors, including mineralogy, degree of angularity, gradations of the materials, and values of σ_3 in the two consecutive triaxial tests.

A careful comparison between Figures 3a and 3b shows that the first stage has more cases with negative values of n . This might indicate that for these materials, comparatively higher particle breakage has happened during the first stage of triaxial testing.

Table 2. Values of n and K parameters for the rockfill materials

Rockfill type	σ_3 (kPa)	n	K	Rockfill type	σ_3 (kPa)	n	K
Railway Ballast-Gradation A-New South Wales-Australia	90 , 120	-7.45	3500	Blasting Lime stone Roodbar Dam	500 , 700	-6.53	18 10 ⁸
	120 , 240	-0.95	1070		700 , 900	-1.15	52000
	90 120, 240	-3.32	2100		500, 700, 900	-3.26	10 10 ⁵
Railway Ballast-Gradation B-New South Wales-Australia	90 , 120	-0.73	3120	Blasting Andesibasalt Sabalan Dam	300 , 600	1.79	71
	120 , 240	-0.79	3120		600 , 900	1.2	203
	90 120, 240	-0.75	3120		300, 600, 900	1.48	178
Masjed-Soleyman,3A Material High Density-Dry	600 , 1200	-0.33	5230	Blasting Andesite Aydoghmosh Dam	300 , 500	1.36	11300
	1200, 1800	0.28	1135		500 , 700	-6.53	36 10 ⁸
	600, 1200, 1800	-0.11	3450		300, 500, 700	-3.2	10 10 ⁵
Masjed-Soleyman,3A Material High Density-Saturated	300 , 600	-0.43	3770	Blasting Sandstone Vanyar Dam	500 , 700	2.6	53
	600 , 1200	0.07	1545				
	300, 600, 1200	-0.22	2340				
Masjed-Soleyman,3A Material Medium Density-Saturated	300 , 600	-0.04	730	Mica granitic- gneiss Dry	500 , 1000	-0.02	1400
	600 , 1200	0.75	175		1000 , 2500	0.16	930
	300, 600, 1200	0.23	340		500, 1000 2500	0.1	1200
San Francisco Basalt Dry	500 , 1000	0.15	1600	Masjed- soleyman,3B Material CU Test,W _{opt} , Gradation B	150 , 300	2.24	1225
	1000, 2500	-0.06	2650		300 , 600	0	14290
	500, 1000, 2500	0.09	1980		150, 300, 600	1.27	8970
Sandstone sample manufactured by Engineering Laboratory Equipment Ltd.	90 , 282	-2.00	12100	Masjed- soleyman,3B Material CU Test,,W _{opt} -2%, Gradation B	150 , 300	-2.21	22300
	282 , 695	0.03	1460		300 , 600	0.46	1180
	90 282, 695	-1.1	9800		150, 300, 600	-1.45	10200
Motorway Embankment Gneiss,Italy Dry	300 , 500	-3.15	16×10 ⁵	Masjed- soleyman,3B Material CD Test,Gradation A	150 , 300	-1.32	5350
	500 , 1000	1.32	1190		300 , 600	0.23	970
	300, 500, 1000	-1.89	8×10 ³		150, 300, 600	-0.6	2130
Limestone Lorestan Roodbar Dam	300 , 500	0.41	4000	Masjed- soleyman,3B Material CU Test,W _{opt} , Gradation A	150 , 300	1.49	750
	500 , 700	-1.28	6×10 ⁴		300 , 600	-2.41	54770
	300, 500, 700	-0.78	20000		150, 300, 600	-0.8	9800
Sandstone Vanyar Dam	300 , 500	-1.16	22430	Masjed- soleyman,3B Material CU Test,,W _{opt} -2%, Gradation A	150 , 300	0.9	315
	500 , 700	1.96	150		300 , 600	-0.28	1150
	300, 500, 700	0.2	3450		150, 300, 600	0.3	650
Andesibasalt& Andesite Sabalan Dam	300 , 600	1.94	60	Ranjit Sagar Dam Dry, d _{max} =25mm	350 , 1400	0.57	215
	600 , 900	0.95	340				
	300, 600, 900	1.3	210				
Dolomite RailRoad Ballast,Coteau,Quebec, Canada	34.4 , 51.7	0.63	755	Ranjit Sagar Dam Dry,d _{max} =50mm	350 , 1400	0.53	330
	51.7 , 310	0.31	610				
	34.4, 51.7, 310	0.52	710				
Purulia Dam Dry,d _{max} =25mm	300 , 1200	0.94	155	Ranjit Sagar Dam Dry,d _{max} =80mm	350 , 1400	0.63	340
Purulia Dam Dry, d _{max} =50mm	300 , 1200	0.71	290	Andesite Yamchi Dam	200 , 400	2.7	1180
					400 , 700	0	5×10 ⁴
					200, 400, 700	1.5	3000
Purulia Dam Dry, d _{max} =80mm	300 , 1200	0.25	790	Andesibasalt Ghale chai Dam	400 , 700	-3.43	2×10 ⁶

Table 3 presents the average values of n for various types of the rockfill materials of this study, compared with typical values for loose and dense sands. As expected, the average n values for each type of the rockfill materials are far less than that of the typical dense sand; it is seen, interestingly, that n decreases with increasing of the materials' angularity.

The main factor responsible for the comparatively lower (compared with sands) average values of n for the rockfill materials (especially the angular ones) is the particle breakage phenomenon which has happened during both compression and shearing of the materials. According to Equation 2, n represents the exponential effect of σ_3 on E_i . As particle breakage in rockfill materials is far more than in sands, the average n values of rockfill materials are much less than those of sands. In general, materials with higher degrees of angularity suffer more particle breakage and therefore, they have lower values of n .

The modulus number (K in Eq. 2) for the studied rockfill

materials takes values ranging widely from 53 to 36×10⁹ (see Table 2). The very high values of K correspond to the negative values of n .

4. Variations of E_i with σ_3/P_a

In this section, variations of the initial elastic modulus with the normalized confining stress in a logarithmic scale ($\log E_i$ versus $\log \sigma_3/P_a$) for the triaxial tests on the studied rockfills are investigated. For this purpose, the materials have been categorized in seven categories of highly angular, angular, angular/sub-angular, sub angular, sub rounded, rounded/sub rounded, and rounded. Our study on one type of the materials (highly angular) is elaborated and described in more details in the paper. For the other six materials types, which for the purpose of brevity the elaborated studies on them aren't presented in this paper, somehow, the same treatment have been observed. Again the main references for the investigation are data of Tables 1 and 2.

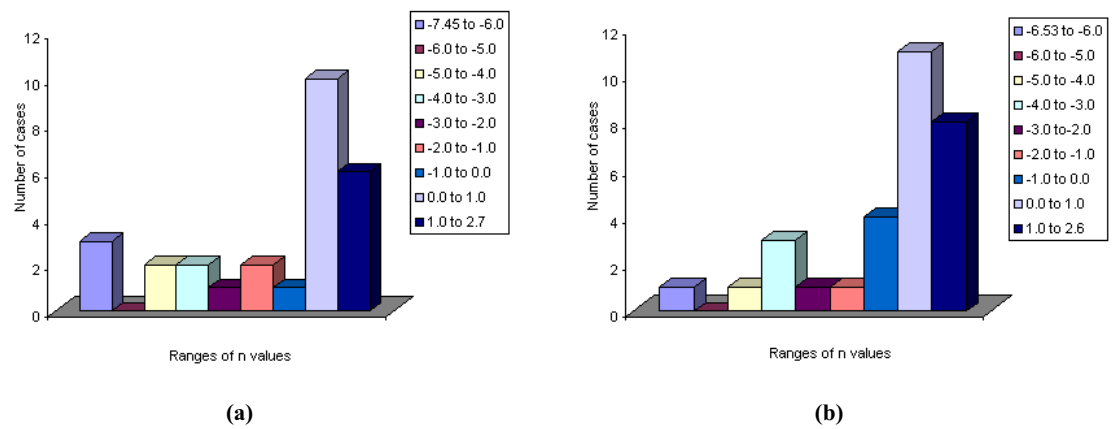


Fig. 3. Statistical variations of n for the rockfill specimens at a) first stage of confining pressure increasing and b) second stage of confining pressure increasing

Table 3. Average values of n for the various types of rockfill materials, compared with typical values for loose and dense sands

Type of Rockfill Materials	n
Highly Angular	0.065
Angular	0.083
Angular/Sub Angular	0.094
Sub Angular	0.11
Sub Rounded	0.18
Rounded/Sub Rounded	0.25
Rounded	0.36
Dense Sands (<i>typical value</i>)	0.54
Loose Sands (<i>typical value</i>)	0.65

4.1. Highly Angular Materials

- New South Wales Basalt

The plots of $\log E_i$ versus $\log \sigma_3/P_a$ for these materials (types A and B) are illustrated in Figure 4. For both of the materials,

the decrease of E_i with the increase of σ_3 is evident. This implies an increasing rate of particle breakage with increasing of confining pressure (σ_3). This relatively high rate of particle breakage can be justified with respect to the particles' angularity and the materials' low uniformity coefficients; C_u equals 1.5 and 1.6 for types A and B materials, respectively. Of course, the exponent number of the Hyperbolic Model (n) takes negative values for the materials for both stages of triaxial testing, as shown in Table 2.

Type A material shows comparatively higher reduction of E_i , particularly during the first stage of confining pressure increase. With respect to the similarity of the mineralogy and C_u of types A and B materials, the difference between the finest particles of the two materials may be thought as the main source of dissimilarity; d_{min} is 20mm for material A and 10mm for material B; hence, A is generally coarser than B. It is physically conceivable that coarser materials are more prone to particle breakage and the coarser the material is, the higher the breakage potential for the material will be. The total values of B_g for materials A and B are 10 and 8.66, respectively (Table 1).

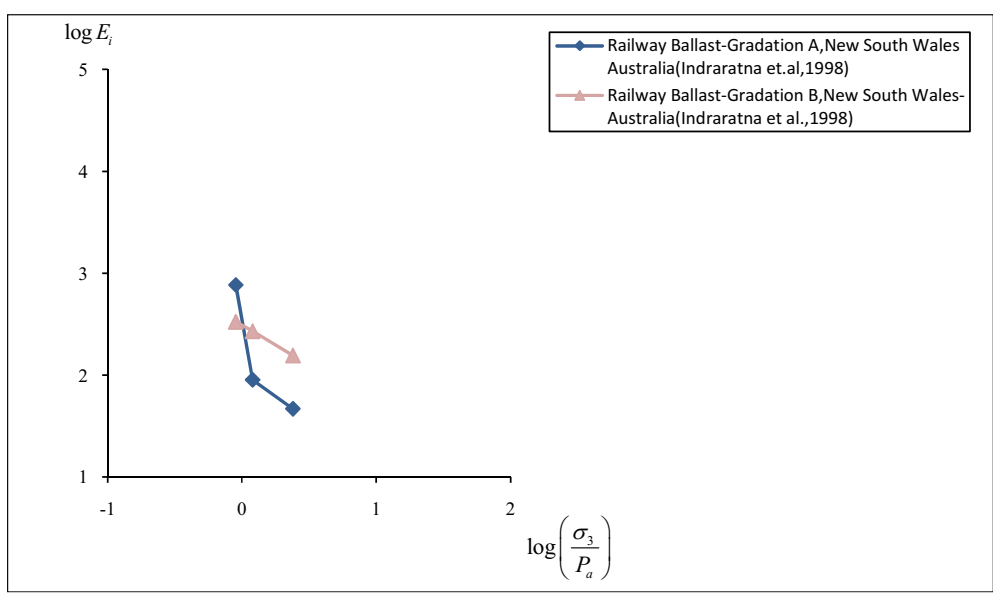


Fig. 4. Variations of $\log E_i$ with $\log(\sigma_3/P_a)$ for the highly angular materials

4. 2. Remarks on Variations of E_i with σ_3/Pa

In the foregoing sections, the effects of confining stress on the initial deformation modulus of 30 rockfill materials were thoroughly studied. In this regard, it should be said that any increase of confining pressure (σ_3) has had two conflicting effects. The application of higher σ_3 values made the materials stiffer (as in soils), on one hand, and induced more particle breakage, on the other hand, that has made the materials more deformable. Particle breakage itself depends on factors such as stress level, gradation (mainly represented by C_u), d_{max} , d_{min} , mineralogy, and shape of the materials.

5. Variations of ϕ with σ_3

It is generally accepted that for all types of rockfill materials (angular and rounded), ϕ decreases with increasing of σ_3 and the intensity of this reduction depends on the extent of particle breakage. The variations of ϕ with confining pressure for seventeen of the rockfill materials (for which ϕ values were available) of this study, have been investigated.

It has been concluded that for all of the materials, ϕ values degrade as the confining pressure increases. For the angular materials, the degradation rate is generally higher since they have suffered more breakage during testing. The maximum reduction of 12 (i.e., 50-38) degrees occurred for ϕ of the sandstone of ELE.

It should be noted that according to Equation 1, particle breakage affects the tangential deformation modulus of rockfill materials by two folds, both by E_i (through n) and by internal friction angle, ϕ . Therefore, it can be concluded that variations of the tangential deformation modulus due to changes of confining pressure in rockfill structures are considerable and must be taken into account in designs and analyses of such structures.

6. Correlation between E_i and ϕ with σ_3

The study on the triaxial testing results of the thirty rockfill materials led to two correlations between E_i and ϕ with σ_3 . These correlations are as follows:

$$\frac{\Delta\phi}{\phi_0} = -\alpha \log\left(1 + \Delta\sigma_3 / \sigma_{30}\right) \quad (3)$$

Where,

$\Delta\phi$: change in internal friction angle

ϕ_0 : internal friction angle corresponding to σ_{30}

σ_{30} : initial confining stress, which is usually the minimum confining stress in triaxial testing.

$\Delta\sigma_3$: confining pressure increase

α : a coefficient depending on particle shape and coefficient of uniformity (C_u) of the material, and confining pressure increment ratio ($\Delta\sigma_3/\sigma_{30}$)

Considering the studied rockfill materials, α ranges between 0.051 and 0.59 for the relatively angular materials and between 0.046 and 0.42 for the relatively rounded materials. Table 4 introduces more specifically five correlations for calculating α for the relatively angular and the relatively rounded materials, based on the particle shape, uniformity

coefficient (C_u), and $\Delta\sigma_3/\sigma_{30}$ in triaxial compression shearing. Here, the highly angular, angular, angular/sub angular, and sub angular materials are assumed as relatively angular materials, while rounded, rounded/sub rounded and sub rounded ones are assumed as relatively rounded materials.

The relationship for variation of E_i with σ_3 is suggested, as follows:

$$\frac{\Delta E_i}{E_{i_0}} = \beta \left(\frac{\Delta\sigma_3}{\sigma_{30}} \right) \quad (4)$$

Where,

ΔE_i : change in initial elasticity modulus

E_{i_0} : initial elasticity modulus corresponding to σ_{30}

β : a coefficient depending on particle shape and coefficient of uniformity (C_u) of the material, and confining pressure increment ratio ($\Delta\sigma_3/\sigma_{30}$).

For the relatively angular materials, β was calculated as $-2.65 \leq \beta \leq 3.71$ and for the relatively rounded materials as $-1.14 \leq \beta \leq 5.50$. It is observed that the range of positive values of β , which implies the increase of E_i with σ_3 , for the relatively angular materials are smaller than the similar range for the relatively rounded materials (3.71 versus 5.50). For the range of negative values of β , which implies the decrease of E_i with σ_3 , the trend is opposite (-2.65 versus -1.14). The above observation is logical, concerning the comparatively higher particle breakage and its reductive effect on E_i for the relatively angular materials. Table 5 introduces more specifically seven correlations for estimating β for the relatively angular and the relatively rounded materials, based on the particle shape, uniformity coefficient of the materials, and ($\Delta\sigma_3/\sigma_{30}$).

7. Conclusions

This paper studied thoroughly the mechanical behavior of thirty rockfill materials subjected to triaxial compression

Table 4. Relationships for calculation of α based on the shape and C_u of the materials and ($\Delta\sigma_3/\sigma_{30}$)

Shape	C_u	Equation
Relatively angular	$C_u < 5.0$	$\alpha = -0.0525(\Delta\sigma_3/\sigma_{30}) + 0.4875$
Relatively angular	$5.0 < C_u < 10.0$	$\alpha = 0.0053(\Delta\sigma_3/\sigma_{30}) + 0.2169$
Relatively angular	$20.0 < C_u < 30.0$	$\alpha = 0.0286(\Delta\sigma_3/\sigma_{30}) + 0.101$
Relatively angular	$C_u > 1000$	$\alpha = -0.0037 (\Delta\sigma_3/\sigma_{30}) + 0.2463$
Relatively rounded	$C_u > 1000$	$\alpha = 0.0026 (\Delta\sigma_3/\sigma_{30}) + 0.1523$

Table 5. Relationships for calculation of β based on the shape and C_u of the materials and ($\Delta\sigma_3/\sigma_{30}$)

Shape	C_u	Equation
Relatively angular	$C_u < 5.0$	$\beta = 0.1412(\Delta\sigma_3/\sigma_{30}) - 0.7636$
Relatively angular	$5.0 < C_u < 10.0$	$\beta = -0.0358(\Delta\sigma_3/\sigma_{30}) + 0.0709$
Relatively angular	$10.0 < C_u < 20.0$	$\beta = -0.0265(\Delta\sigma_3/\sigma_{30}) + 0.7559$
Relatively angular	$20.0 < C_u < 30.0$	$\beta = 0.0638(\Delta\sigma_3/\sigma_{30}) + 0.1818$
Relatively angular	$C_u > 1000$	$\beta = -0.3208(\Delta\sigma_3/\sigma_{30}) + 1.4983$
Relatively rounded	$50.0 < C_u < 200.0$	$\beta = -0.0698(\Delta\sigma_3/\sigma_{30}) + 0.9716$
Relatively rounded	$C_u > 1000$	$\beta = -0.0269(\Delta\sigma_3/\sigma_{30}) + 0.0029$

shearing with three different confining stresses. Data about the materials and the triaxial tests were collected all from the literature. Accordingly, most of the tests (76 out of 88) had been carried out in consolidated (CD) drained conditions. The Hyperbolic Model was employed as the behavioral model for this study. Features of the mechanical behavior of the rockfill materials, as compared with the typical behavior of soils, were highlighted through the exponent number (n) of the Hyperbolic Model. It was shown that unlike for soils, n is not a constant value for a given rockfill material, and depends on confining stress levels; it was also illustrated that n , depending on the rockfill type and stress level, can even take negative values that is an evident sign of particle breakage in the materials.

The main focus of the paper was on the effect of confining pressure on the stiffness (initial and tangential deformation modulus E_i and E_t) of the materials. It was shown that rockfill materials undergo particle breakage to some extents and therefore, they may behave comparatively more deformable than soils under higher confining stresses. The extent of particle breakage in a rockfill material depends on particle shape (angular or rounded), gradation characteristics, (especially coefficient of uniformity), wetting conditions, and confining stress during shearing.

For the studied rockfill materials two correlations for estimating initial elasticity modulus (E_i) and internal friction angle (φ), based on particles shape, confining pressure (σ_3), and coefficient of uniformity (C_u) were proposed. Investigations on the variations of internal friction angle (φ) with confining stress (σ_3) showed that φ decreases with increasing of σ_3 in all types of the rockfill materials; the extent of the reduction of φ depends on the extent of particle breakage.

References

- [1] Baziar, M. H. , Salemi, Sh. and Heidari, T. (2006), "Analysis of Earthquake Response of an Asphalt Concrete Core Embankment Dam", International Journal of Civil Engineering, Volume 4, Number 3
- [2] Salehzadeh, H. , Procter, D. C. and Merrifield, C. M. (2005), " A Carbonate Sand Particle Crushing Under Monotonic Loading", International Journal of Civil Engineering, Volume 3, Number 3
- [3] Hassanlourad, M. , Salehzadeh, H. and Shahnazari, H. (2008), " Dilation and Particle Breakage Effects on the Shear Strength of Calcareous Sands Based on Energy Aspects", International Journal of Civil Engineering, Volume 6, Number 2
- [4] Marsal, R.J. (1972), "Mechanical Properties of Rockfill in Embankment Dam Engineering", Casagrande Volume, Wiley & Sons, New York, p.109-200
- [5] Soltani- Jigheh, H. and Soroush. A. (2010), " Cyclic Behavior of Mixed Clayey Soils", International Journal of Civil Engineering, Volume 8, Number 2
- [6] Soltani- Jigheh, H. and Soroush. A. (2006), " Post-cyclic Behavior of Compacted Clay- sand Mixtures", International Journal of Civil Engineering, Volume 4, Number 3
- [7] Duncan, J. M. and Chang, Ch. Y. (1970), " Nonlinear Analysis of stress and strain in soils", Journal of soil mechanics and foundations division, p.1629-1653
- [8] Konder, R. L. (1963) " Hyperbolic Stress-Strain Response: Cohesive Soils" Journal of the soil mechanics and foundations division, ASCE, Vol.89, No.1, Proc. paper, p.115-143

- [9] Janbu, N. (1963), "Soil Compressibility as determined by Oedometer and triaxial tests," European Conference on Soil Mechanics and Foundations Engineering, Wiesbaden, Germany, Vol. 1, p. 19-25
- [10] Varadarajan, A. , Sharma, K.G. ,Venkatachalam, K. and Gupata, A. K. (2003), "Testing and Modeling Two Rockfill Materials", Journal of Geotechnical and Geoenvironmental Engineering , March 2003, p. 206-218
- [11] Brauns, J. (1993), "Laboratory Tests Report on Materials of Masjed Soleyman Dam", Division of Earth Dam and Landfill Technology, University of Karlsruhe
- [12] Charles, J.A. and Watts, K.S. (1980), "The influence of confining pressure on the shear strength of compacted rockfill", Geotechnique 30, No.4, p.353-367
- [13] Frassoni, A., Hegg, U. and Rossi, P. (1982), "Large-scale laboratory tests for the mechanical characterization of granular materials for embankment dams", Proc. Congres des Grands Barrages, Rio de Janeiro, p.727-751
- [14] Indraratna, B., Ionescu, D., and Christie, H.D. (1998), "Shear behavior of railway ballast based on large-scale triaxial tests." J. SMFE, ASCE, 124(5), p. 439-449
- [15] Raymond, J. P. (1978), " Behavior of Dolomite Railroad Ballast of Coteau, Canada, under Large Scale Triaxial Testing" ,Geotechnique26, No.2, p.257-276
- [16] Moshanir Power Engineering Consultants, (1996), Review on Additional Laboratory Tests on Materials of Masjed Soleyman Dam, , Tehran, Iran
- [17] Tofigh Rayhani M.H. (2000). "Studying the mechanical behavior of rockfill and earth dam faces using large scale triaxial and direct shear test", M.Sc. Thesis, Tarbiat Moallem University, Tehran, Iran
- [18] BHRC (1994-2006), "Testing of rockfill materials with large-scale triaxial equipment", TP, Geotechnical Department

Notation

- d_{min} : the finest grain size (mm)
 d_{max} : the largest grain size (mm)
 C_u : coefficient of uniformity
 σ_3 : confining stress (kPa)
 φ : internal friction angle (degree)
 B_g : Marsal's breakage index (%)
 CD: Consolidated drained triaxial test
 CU: Consolidated Undrained triaxial test
 ω_{opt} : optimum moisture
 c : cohesion
 K : modulus number
 n : exponent number
 P_a : atmospheric pressure
 E_i : initial elastic modulus
 σ_3/P_a : normalized confining stress
 $\Delta\varphi$: reduction of internal friction angle
 φ_0 : internal friction angle corresponding to σ_{30}
 σ_{30} : initial confining stress, which is usually the minimum confining stress in triaxial testing
 $\Delta\sigma_3$: confining pressure increase
 α : a coefficient depending on shape of particles, coefficient of uniformity (C_u), and confining pressure increment ratio ($\Delta\sigma_3/\sigma_{30}$).
 ΔE_i : change in initial elasticity modulus
 E_{i0} : initial elasticity modulus corresponding to σ_{30}
 β : a coefficient depending on particle shape, uniformity coefficient (C_u), and $\Delta\sigma_3/\sigma_{30}$ in triaxial compression shearing.